Inorg. Chem. **2003**, *42*, 7026–7036

A Solid-State Spectral Effect in Eclipsed Tetracyanonickelates: X-ray Crystal Structure, Polarized Specular Reflectance Spectroscopy, and ZINDO Modeling of $Sr[Ni(CN)_4]\cdot 5H_2O$, $Rb_2[Ni(CN)_4]\cdot H_2O$, and $Na_2[Ni(CN)_4]\cdot 3H_2O$

Frank R. Fronczek, Terry J. Delord, Steven F. Watkins, Petia Gueorguieva, and George G. Stanley

Department of Chemistry, Louisiana State University, Baton Rouge, Louisiana 70803

Annegret S. Zizza and Jeffrey B. Cornelius

Department of Chemistry, Principia College, Elsah, Illinois 62028

Yves A. Mantz[†] and Ronald L. Musselman*

Department of Chemistry, Franklin and Marshall College, Lancaster, Pennsylvania 17604

Received May 15, 2003

Crystal structures of three $Ni(CN)_4^{2-}$ salts all with eclipsed ligands and varying axial stacking arrangements are presented. The absorption spectra of all three salts show a slight red shift in the *x*,*y*-polarizations and a large red shift in their *z*-polarizations upon crystallization from solution. Semiempirical ZINDO calculations provide a good model of the solid state, even with only a three-molecule segment, allowing reproduction of the red-shifting and intensity increase upon crystallization found experimentally. The modified nickel $\beta_{s,p}$ bonding parameter of –5 found appropriate for Ni coordination in our previous studies of single $Ni(CN)_4^{2-}$ planes and a helically stacked $Cs_2[Ni(CN)_4]\cdot H_2O$ crystal was changed to –3 for the more parallel-stacked $Ni(CN)_4^{2-}$ planes in this case, while β_d was retained at –41. Crystal data are as follows: $Na_2[Ni(CN)_4]\cdot 3H_2O$, triclinic space group $P\bar{1}$, $a = 7.2980(10)$ Å, $b = 8.8620(10)$ Å, $c = 15.132(2)$ Å, $\alpha = 89.311(5)°$, $\beta = 87.326(5)°$, $\gamma = 83.772(6)°$, $V = 971.8(2)$ Å^3, $T = 100$ K, $Z = 4$, $R = 0.024$, $R_w = 0.064$; $Sr[Ni(CN)_4]\cdot 5H_2O$, monoclinic space group $C2/m$, $a = 10.356(2)$ Å, $b = 15.272(3)$ Å, $c = 7.1331(10)$ Å, $\beta = 98.548(12)°$, $V = 1115.6(3)$ Å^3, $T = 100$ K, $Z = 4$, $R = 0.024$, $R_w = 0.059$; $Rb_2[Ni(CN)_4]\cdot 1.05H_2O$, triclinic space group $P\bar{1}$, $a = 8.6020(10)$ Å, $b = 9.6930(10)$ Å, $c = 12.006(2)$ Å, $\alpha = 92.621(6)°$, $\beta = 94.263(6)°$, $\gamma = 111.795(10)°$, $V = 924.0(2)$ Å^3, $T = 100$ K, $Z = 4$, $R = 0.034$, $R_w = 0.067$.

Introduction

Square-planar nickel complexes have been known to form colored solids from colorless solutions since at least 1905 when Tschugeaff described a gravimetric test for nickel using dimethylglyoxime (dmg).[1,2] The resultant $Ni(dmg)_2$ is the familiar brilliant crimson precipitate that precipitates quantitatively. The spectral perturbation upon crystallization in $Ni(dmg)_2$ was studied by several individuals in the middle of the 20th century.[3–8] Anex and Krist[7] found a correlation between adjacent stacked planes and the degree of red-shift from the UV region in solution for the prominent absorption peak in the green portion of the spectrum of solid $Ni(dmg)_2$. Tetracyano complexes of nickel show a similar spectral perturbation,[9,10] but the shifted peak remains in the UV

* To whom correspondence should be addressed. E-mail: ronald.musselman@fandm.edu.

[†] Current address: IBM T. J. Watson Research Center, P.O. Box 218, Yorktown Heights, NY 10598-0218.

(1) Tschugeaff, L. *Z. Anorg. Chem.* **1905**, *46*, 144.
(2) Tschugeaff, L. *Ber. Dtsch. Chem. Ges.* **1905**, *38*, 2520.
(3) Banks, C. V.; Barnum, D. W. *J. Am. Chem. Soc.* **1958**, *80*, 4767.
(4) Banks, C. V.; Barnum, D. W. *J. Am. Chem. Soc.* **1958**, *80*, 3579.
(5) Zahner, J. C.; Drickamer, H. G. *J. Chem. Phys.* **1960**, *33*, 1625.
(6) Basu, G.; Cook, G. M.; Belford, R. L. *Inorg. Chem.* **1964**, *3*, 1361.
(7) Anex, B. G.; Krist, F. K. *J. Am. Chem. Soc.* **1967**, *89*, 6114.
(8) Yamada, S.; Tsuchida, R. *Bull. Chem. Soc. Jpn.* **1954**, *27*, 156.

10.1021/ic0345222 CCC: $25.00
Published on Web 09/27/2003

Table 1. Elemental Analysis of $M[Ni(CN)_4]\cdot xH_2O$ (in %)

M $[Ni(CN)_4]$		M	Ni	C	N	H	O	Ba	K
$Sr[Ni(CN)_4]\cdot 5H_2O$	calcd	25.73	17.24	14.11	16.46	2.97	23.49		0.0
	found	26.00	17.42	13.94	16.31	2.93	23.44		<0.008
$Rb_2[Ni(CN)_4]\cdot 1.05H_2O$	calcd	48.35	16.60	13.59	15.85	0.60	4.75	0.0	
	found	52.67	17.52	13.74	15.76	0.56	<0.5	<0.1	
$Na_2[Ni(CN)_4]\cdot 3H_2O$	calcd	17.50	22.35	18.28	21.32	2.29	18.27	0.0	
	found	17.25	22.53	18.01	21.11	2.35	18.42	<0.08	

portion of the spectrum and the red shift is thus not visible. The crystal structures of square-planar nickel and platinum complexes produce a one-dimensional collective effect that has proven to be useful in several applications.[11−13] Our principal interest has been to identify the mechanism of spectral perturbation and its relationship to metallic conductivity and other electronic effects in the solid state.[9,11,14−23] The perturbation has been described by some as band formation,[24] while others have suggested exciton formation.[25] We have long suspected that the phenomenon is neither of these.[15]

We previously demonstrated that in stacked planar tetracyanometalates there is an extended perturbation of some sort, extending over at least 20 metal centers, using mixed-metal stacks of $M(CN)_4^{2-}$ in crystals prepared from mixtures of $Ba[Ni(CN)_4]\cdot 4H_2O$ and $Ba[Pt(CN)_4]\cdot 4H_2O$ with from 5% to 95% $Ba[Pt(CN)_4]\cdot 4H_2O$.[15] At all concentrations, a single out-of-plane-polarized a_{1g} (d_{z^2}) → a_{2u} (p_z, π^*) transition was found whose intensity and energy were proportional to composition as % Pt or Ni. We have recently returned to the issue of the electronic structure of stacked planes of tetracyanonickelates; in our initial paper,[26] we calculated the electronic structure of the isolated $Ni(CN)_4^{2-}$ anion using the semiempirical technique, ZINDO, and in a subsequent paper, we have studied a helically stacked solid, $Cs_2[Ni(CN)_4]\cdot H_2O$.[10] In the former case, we demonstrated that with reasonable parameter adjustment, the single-ion polarized spectrum could be modeled with excellent accuracy in both energy and transition intensity. In the latter case, we showed that, by using the same parameters as found for the single $Ni(CN)_4^{2-}$ ion, the red-shifts in both the in-plane and out-of-plane spectra could be modeled very well with the simple linear-combination-of-atomic-orbitals approach used by the ZINDO routine.

Tetracyanonickelate salts have several different structures, with stacked $Ni(CN)_4^{2-}$ planes in various arrangements and with different stacking distances. The stacking arrangements include the helical one of $Cs_2[Ni(CN)_4]\cdot H_2O$,[10] parallel planes with 45° alternating arrangements of CN^- ligands ("staggered"),[27,28] and essentially parallel planes with eclipsed ligands. In this work, we have chosen three salts with the latter arrangement: $Sr[Ni(CN)_4]\cdot 5H_2O$, $Rb_2[Ni(CN)_4]\cdot H_2O$, and $Na_2[Ni(CN)_4]\cdot 3H_2O$. Our goal is to understand axial perturbation in a system with maximum overlap of orbitals from adjacent planes. Neither X-ray structures nor polarized spectroscopy have been available for this system, so we began with the collection of those and then performed semiempirical calculations to model these systems.

Experimental Section

Preparation. $Sr[Ni(CN)_4]\cdot 5H_2O$. A saturated solution of 6.86 g of $K_2Ni(CN)_4\cdot 3H_2O$ in 99 mL of distilled water was added to a saturated solution of 62.02 g of $SrCl_2\cdot 6H_2O$ (a 10-fold molar excess) in 83 mL distilled water. This solution was heat evaporated for a day until it became cloudy. The precipitate was gravity filtered, and heat evaporation was resumed; the process was repeated until the volume became about 100 mL. The solution was cooled slowly, and the resulting orange crystals (2.67 g) were harvested and recrystallized from 10 mL of distilled water in a desiccator. After 6 days, well-formed small (1 × 1 × 2 mm) crystals of $Sr[Ni(CN)_4]\cdot 5H_2O$ had formed. Elemental analysis was performed by Galbraith Laboratories, Knoxville, TN; the results shown in Table 1 show that essentially no K^+, which would be the most likely contaminant, remained.

$Rb_2[Ni(CN)_4]\cdot H_2O$. A solution of 15 mL of deionized water and 5.00 g of Rb_2SO_4 was added to a solution of 80 mL of water and 6.95 g of $Ba[Ni(CN)_4]\cdot 4H_2O$, prepared as described earlier.[9] The combined solutions were stirred for 1 day and filtered with a fine sintered glass filter. The filtrate was heat evaporated to about 15 mL and covered and allowed to cool slowly. After 24 h, there were many well-formed orange needlelike crystals. Analysis shows essentially no Ba^{2+} remained, as shown in Table 1. Using the value of 1.05 waters as found by our X-ray structure determination (vide infra), most of the values show a good match between calculated and found compositions. We found in the X-ray study that one of the waters was present approximately 20% percent of the time,

(9) Musselman, R. L.; Cornelius, J. B.; Trapp, R. M. *Inorg. Chem.* **1981**, *20*, 1931.
(10) Cornelius, J. B.; Trapp, R. M.; Delord, T. J.; Fronczek, F. R.; Watkins, S. F.; Orosz, J. J.; Musselman, R. L. *Inorg. Chem.* **2003**, *42*, 3026.
(11) Musselman, R. L.; Williams, J. W. *J. Chem. Soc., Chem. Commun.* **1977**, 186.
(12) McHale, G.; Newton, M. I.; Hooper, P. D.; Willis, M. R. *Opt. Mater.* **1996**, 89.
(13) Flamini, A.; Poli, N. *Sens. Mater.* **1995**, *7*, 99.
(14) Johnson, P. L.; Musselman, R. L.; Williams, J. M. *Acta Crystallogr., Sect. B* **1977**, *33*, 3155.
(15) Anex, B. G.; Musselman, R. L. *J. Phys. Chem.* **1980**, *84*, 883.
(16) Musselman, R. L.; Stecher, L. C.; Watkins, S. F. *Inorg. Chem.* **1980**, *19*, 3400.
(17) Musselman, R. L.; Anex, B. G. *J. Phys. Chem.* **1987**, *91*, 4460.
(18) Arndt, G. A.; Danielson, E. D.; Fanta, A. D.; Musselman, R. L. *Inorg. Chem.* **1988**, *27*, 1400.
(19) Heagy, M. D.; Rende, D. E.; Shaffer, G. W.; Wolfe, B. M.; Liou, K.; Hoffman, B. M.; Musselman, R. L. *Inorg. Chem.* **1989**, *28*, 283.
(20) Liang, X.; Flores, S.; Ellis, D. E.; Hoffman, B. M.; Musselman, R. L. *J. Chem. Phys.* **1991**, *95*, 403.
(21) Rende, D. E.; Heagy, M. D.; Heuer, W. M.; Liou, K.; Thompson, J. A.; Hoffman, B. M.; Musselman, R. L. *Inorg. Chem.* **1992**, *31*, 352.
(22) Liou, K. Y.; Newcomb, T. P.; Heagy, M. D.; Thompson, J. A.; Heuer, W. B.; Musselman, R. L.; Jacobsen, C. S.; Hoffman, B. M.; Ibers, J. A. *Inorg. Chem.* **1992**, *31*, 4517.
(23) Liang, X. L.; Ellis, D. E.; Gubanova, O. V.; Hoffman, B. M.; Musselman, R. L. *Int. J. Quantum Chem.* **1994**, *52*, 657.
(24) Whangbo, M. H.; Hoffman, R. *J. Am. Chem. Soc.* **1978**, *100*, 6093.
(25) Day, P. *J. Am. Chem. Soc.* **1975**, *97*, 1588.
(26) Mantz, Y. A.; Musselman, R. L. *Inorg. Chem.* **2002**, *41*, 5770.
(27) Larsen, F. K.; Hazell, R. G.; Rasmussen, S. E. *Acta Chem. Scand.* **1969**, *23*, 61.
(28) Dowling, J. P. *Acta Chem. Scand.* **1992**, *23*, 14.

Table 2. Crystal Data and Data Collection and Refinement Parameters

	sodium salt	strontium salt	rubidium salt
formula	$Na_2[Ni(CN)_4]\cdot 3H_2O$	$Sr[Ni(CN)_4]\cdot 5H_2O$	$Rb_2[Ni(CN)_4]\cdot 1.05H_2O$
color/shape	yellow fragment	golden-yellow fragment	golden-yellow fragment
fw	262.8	340.5	352.7
cryst syst	triclinic	monoclinic	triclinic
space group	$P\bar{1}$	$C2/m$	$P\bar{1}$
T, K	100	100	100
cell constants			
a, Å	7.2980(10)	10.356(2)	8.6020(10)
b, Å	8.8620(10)	15.272(3)	9.6930(10)
c, Å	15.132(2)	7.1331(10)	12.006(2)
α, deg	89.311(5)		92.621(6)
β, deg	87.326(5)	98.548(12)	94.263(6)
γ, deg	83.772(6)		111.795(10)
V, Å^3	971.8(2)	1115.6(3)	924.0(2)
formula units/unit cell	4	4	4
D_{calcd}, g cm^{-3}	1.796	2.027	2.535
μ_{calcd}, cm^{-1}	20.7	64.8	125.2
transm coeff	0.681−0.813	0.309−0.523	0.179−0.222
diffractometer/scan	Nonius KappaCCD/ω	Nonius KappaCCD/ω	Nonius KappaCCD/ω
radiation, graphite monochromated	Mo Kα ($\lambda = 0.71073$ Å)	Mo Kα ($\lambda = 0.71073$ Å)	Mo Kα ($\lambda = 0.71073$ Å)
max cryst dimensions, mm^3	0.10 × 0.18 × 0.21	0.10 × 0.20 × 0.20	0.12 × 0.15 × 0.17
reflns measured	34 807	29 323	30 158
R_{int}	0.018	0.018	0.026
indep reflns	8269	2619	8380
2θ range, deg	$5.0 < 2\theta < 70.0$	$5.0 < 2\theta < 71.2$	$5.0 < 2\theta < 74.0$
range of h, k, l	±11, ±14, ±24	±16, ±24, ±11	±13, ±15, ±19
reflns obsd	7223	2426	6902
criterion for obsd	$I > 2\sigma(I)$	$I > 2\sigma(I)$	$I > 2\sigma(I)$
data/params	8269/293	2619/99	8380/228
R(obsd)	0.024	0.024	0.034
R(all data)	0.030	0.027	0.049
R_w, F^2(all data)	0.064	0.059	0.067
GOF	1.02	1.07	1.04
max residual peaks (e Å^{-3})	0.74, −0.73	1.14, −0.72	2.11, −1.48

suggesting that this water is easily lost from the crystal. The very low value for oxygen may well be due to water loss during analysis. During handling of samples for spectroscopy and single-crystal X-ray film work, the crystals exhibited a tendency to lose water. Samples were stored under a relative humidity of 58%, achieved via a saturated NaBr solution.

$Na_2[Ni(CN)_4]\cdot 3H_2O$. Stoichiometric amounts of $Ba[Ni(CN)_4]\cdot 4H_2O$ (5.00 g), and $Na_2SO_4\cdot 10H_2O$ (4.53 g) were dissolved in 60 mL and 30 mL, respectively, of deionized water. The solutions were combined and heated for 3 h. Upon filtering out the precipitated $BaSO_4$, the filtrate was evaporated to 8 mL and then covered and allowed to cool slowly for 24 h. A total of 1.44 g of well-formed orange crystals was harvested. Elemental analysis by Galbraith Laboratories showed the product to be free of Ba; details are shown in Table 1. The crystal used for the X-ray structure determination was isolated as a side product of cyanolysis of the Ni tetraphosphine complex *rac*-$Ni_2Cl_4(Me_2PCH_2CH_2)(Ph)PCH_2P(Ph)(CH_2CH_2PMe_2)$. Diffraction-quality crystals formed from wet benzene solution over one month.

X-ray Data Collection and Structure Determination. Intensity data were collected for the three compounds using graphite monochromated Mo Kα radiation ($\lambda = 0.71073$ Å) on a Nonius KappaCCD diffractometer fitted with an Oxford Cryostream cooler. Data reduction included absorption corrections by the multiscan method. Crystal data and experimental details are given in Table 2. Structures were solved by direct methods and refined by full-matrix least squares, using SHELXL97.[29] For the Na^+ and Sr^{2+} salts, all H atoms were located in difference maps and individually refined. For the Rb^+ salt, H atoms could not be located, and electron density at 0, 0, 0 was interpreted as partial occupancy of a water molecule, O3. Its population parameter was refined to a value of 0.197(3).

Spectral Measurements. Due to the high spectral extinction coefficients for this system, room-temperature polarized spectra were obtained through specular reflectance rather than transmission. The reflectance instrument, based on a concept by Anex,[30] was essentially a grating microspectrophotometer consisting of tungsten-halogen and xenon arc light sources, an Instruments SA HR320 0.32 m computer controllable grating monochromator, a Glan-Thompson polarizer, a double-beam reflecting microscope, and a photomultiplier detector. Signal detection was through two Princeton Applied Research 186A lock-in amplifiers, and instrument control resided on an Apple IIe computer. The data were uploaded to a Hewlett-Packard 3000 computer for processing. Reflectance was measured relative to a NIST standard second-surface mirror. Kramers-Kronig transformation[30,31] of the reflectance data provided standard absorbance values. Since Kramers-Kronig transformation requires reflectance data over energies from 0 to ∞, an effective transition was added at energies higher than the experimental region and adjusted so that the valleys in the transformed data resembled those from solution data. We assumed that the infrared reflectance was constant and at the level of the lowest-energy measured reflectances for both compounds; effective transition reflectances used were equivalent to those reported earlier.[10] Polarized single-crystal specular reflectance spectra were taken on natural faces with the electric vectors parallel to and perpendicular to the needle direction, unless described otherwise in the spectral results.

Crystalline samples were kept under moist conditions (~50% relative humidity) during the collection of reflectance spectra to

(29) Sheldrick, G. M. *SHELXL97*; University of Göttingen: Germany, 1997.

(30) Anex, B. G. *Mol. Cryst.* **1966**, *1*, 1.

(31) Kronig, R. *J. Opt. Soc. Am.* **1926**, *12*, 547.

avoid loss of waters of crystallization and subsequent degradation of surface reflectance. Solution spectra were obtained on a Perkin-Elmer Lambda 40 UV-vis spectrophotometer at room temperature.

Semiempirical Calculations. Ground state energies, molecular orbitals, and allowed electronic transitions for units of two and three planes at various interplanar spacings, including that for $Sr[Ni(CN)_4]\cdot 5H_2O$, were calculated using the Zerner-modified semiempirical INDO (intermediate neglect of differential overlap) method known as ZINDO.[32] The version of ZINDO we use here is contained in the CAChe suite of programs from Fujitsu.[33] It has been extremely successful in calculating theoretical electronic spectra of the dianion, $Ni(CN)_4^{2-}$,[26] and the helically stacked solid, $Cs_2[Ni(CN)_4]\cdot H_2O$,[10] as well as numerous porphyrinic complexes.[34−37]

Because the ZINDO technique is semiempirical, the calculation parameters typically need to be optimized in order for the calculated electronic spectrum to match the experimental spectrum as closely as possible. We are expecting that the values of the parameters will reflect the behavior of the valence electrons in the extended systems. The CAChe implementation of ZINDO includes default values for numerous parameters.[26] The parameters most commonly adjusted in transition metal complexes are the bonding parameters for the central metal, β_s, β_p, and β_d.[38] β_s and β_p are set equal ("$\beta_{s,p}$") and represent the amount of interaction between occupied s and p orbitals on the metal with atomic orbitals on adjacent atoms; β_d is similarly defined. Values that are more negative represent a greater interaction between the corresponding metal orbital(s) and the ligand orbitals. We used the optimized β parameters from our recent work[26] on the single $Ni(CN)_4^{2-}$ ion as starting parameters in this current work: $\beta_{s,p} = -5$ and $\beta_d = -41$ (all β values have units of au), but made a limited modification upon detailed evaluation of the results. In determining transition energies, ZINDO uses a process known as configuration interaction (CI). The CI process in ZINDO considers the effects of single-electron excitations from a set of filled orbitals to a set of virtual orbitals. The "CI level" is an integer representing the number of orbitals in each region used in the CI calculation. Since the ZINDO CI in CAChe includes only single excitations, the choice of CI level in this case affects only the state transitions and not the individual orbital energies or wave functions.[26] In the single dianion paper,[26] we found that a CI level of 10 was the maximum suitable for all transitions but that the *z*-polarized transitions could be accurately modeled with a CI level of 6.

In the CAChe implementation, the maximum CI level is 22, so *z*-polarized transitions are accurately calculable for aggregations up to three. The *x*,*y*-polarized transitions would formally need a CI level of 30 for a set of three, but we found good agreement with experiment in the helical $Cs_2[Ni(CN)_4]\cdot H_2O$[10] using the CI = 22 available in the routine and we will therefore assume that CI = 22 will be appropriate for stacks of three in the systems under study here also.

(32) Ridley, J.; Zerner, M. *Theor. Chim. Acta* **1973**, *32*, 111.
(33) Zerner, M. C. *ZINDO (in CAChe)*; Fujitsu Limited: Beaverton, OR, 2000.
(34) Edwards, W. D.; Weiner, B.; Zerner, M. C. *J. Am. Chem. Soc.* **1986**, *108*, 2196.
(35) Vitasovic, M.; Gouterman, M.; Linschitz, H. *J. Porphyrins Phthalocyanines* **2001**, *5*, 191.
(36) Mack, J.; Stillman, M. J. *Inorg. Chem.* **1997**, *36*, 413.
(37) Evans, J. S.; Musselman, R. L. *Abstracts of Papers*, 225th National Meeting of the American Chemical Society, New Orleans, LA, 2003; American Chemical Society: Washington, DC; INOR363.
(38) Anderson, W. P.; Edwards, W. D.; Zerner, M. C. *Inorg. Chem.* **1986**, *25*, 2728.

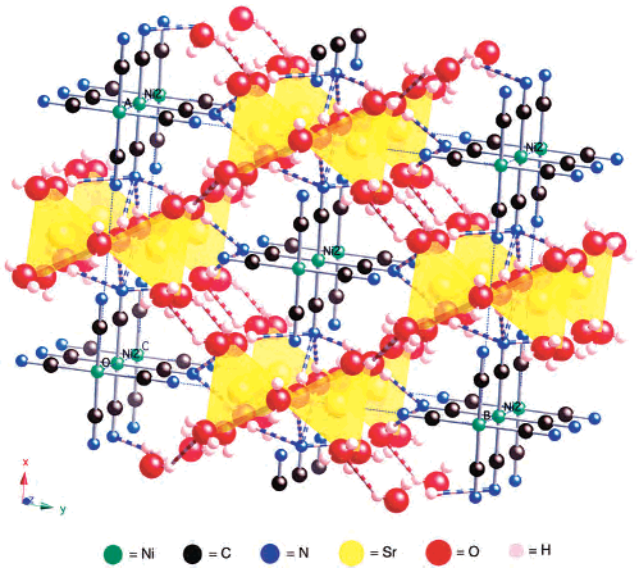

Figure 1. Structure of $Sr[Ni(CN)_4]\cdot 5H_2O$. Translucent shapes = Sr coordination prisms and blue/pink bonds = hydrogen bonds.

Results

Description of the Structures. All three structures have stacks of eclipsed $Ni(CN)_4^{2-}$ ions surrounded by cations and water molecules. The structure of the chain differs among the three structures as does the geometry of coordination of the cations.

$Sr[Ni(CN)_4]\cdot 5H_2O$. The crystal structure of $Sr[Ni(CN)_4]\cdot 5H_2O$ consists of columns of planar $Ni(CN)_4^{2-}$ ions aligned along a straight line with their plane normals tilted an average of 15.3° from the stacking vector. The Sr^{2+} ions are coordinated only to water molecules; the coordination polyhedra are arranged in pairs with hydrogen bonding between them. Hydrogen bonding also occurs between half of the $Ni(CN)_4^{2-}$ planes and some water molecules as shown in Figure 1; detailed descriptions follow. Crystallographic details are in the Supporting Information.

(a) $Ni(CN)_4^{2-}$. There are two independent anions, both of which are close to being planar. The anion containing Ni1 is tilted 15.93(1)° to the stack (*z*) axis, while that containing Ni2 is tilted 14.63(1)° to the stack axis. The dihedral angle formed by the two anion planes is 2.24(3)°. C−Ni−C angles are constrained by symmetry to be 90°. Two of the four independent N−C−Ni angles are 180°, and the other two are 177.48(17)° and 177.14(17)°, with the N bent slightly out of the plane. The mean Ni−C and C−N distances are 1.858 and 1.159 Å, respectively, comparable to previous observations.[26,27] The Ni−Ni distance is 3.567(2) Å, and the interplanar distance is 3.440(2) Å. The nitrogens on only one of the two $Ni(CN)_4^{2-}$ planes (Ni2) are hydrogen bonded to surrounding water molecules. The N22's point toward the centers of a stack of Sr^{2+} coordination pairs and are hydrogen bonded to the O3's on two different pairs and to two O2's on opposite ends of one of the Sr^{2+} coordination pairs. The N21's point toward the single sides of a set of stacked coordination prisms and are hydrogen bonded to a pair of O2's, each from different prisms.

Table 3. Hydrogen Bonding

O−H−X	OHX bond angle, deg	distance, Å O−H	distance, Å H−X
	$Sr[Ni(CN)_4]\cdot 5H_2O$		
O1−H1A−O2	141(2)	0.77(3)	2.36(3)
O2−H2B−N22	156(3)	0.75(3)	2.51(3)
O3−H3B−N22	178(3)	0.80(3)	2.08(3)
O3−H3A−N22	175(3)	0.86(3)	1.95(3)
O2−H2A−N21	177(3)	0.78(3)	2.12(3)
	$Na_2[Ni(CN)_4]\cdot 3H_2O$		
O1−H1A−N6	155.6(16)	0.786(18)	2.335(18)
O1−H1B−N3	159.6(16)	0.780(18)	2.410(17)
O3−H3A−N5	165.5(15)	0.793(16)	2.180(16)
O4−H4B−N6	164.7(14)	0.826(16)	2.152(16)
O4−H4A−N6	157.0(15)	0.775(16)	2.546(16)
O6−H6A−N4	168.8(16)	0.792(17)	2.126(17)
O6−H6B−N2	126.4(13)	0.809(17)	2.670(16)

(b) Sr^{2+}. Each Sr^{2+} is tightly coordinated to six O atoms in a slightly distorted trigonal prism configuration with bond distances of 2.58−2.62 Å. The coordination prisms are depicted as yellow translucent objects in the figure. The Sr^{2+}'s are paired, with the coordination prisms joined at the edge with two O3 atoms, as shown in Figure 1. The pairs of coordination prisms are isolated from others in the structure; that is, they share no common O atoms with other pairs, but all of the water molecules are hydrogen bonded to the O's on nearby Sr^{2+}'s. Thus, rings of six coordination polyhedra linked either through common O atoms or hydrogen bonded O's surround each stack of $Ni(CN)_4^{2-}$ ions. There is no coordination from Sr^{2+} directly to N atoms.

(c) H_2O. As noted, there are hydrogen bonds from N's to H_2O and H_2O to H_2O. The N−H bond lengths range from 1.94(3) to 2.51(3) Å, with N−H−O bond angles from 156(3)° to 177(3)°. There is only one type of hydrogen bond between water molecules: from O2 to H1A, with an O2−H1A length of 2.36(3)Å and an O−H−O angle of 141(2)°. A complete listing is given in Table 3.

(d) Crystal Morphology. The crystals formed as needles with the (001) axis (*c*) as the needle axis and an approximately hexagonal cross-section. The most prominent elongated faces were the (110) and the $(\bar{1}\bar{1}0)$ planes, and the other four faces were (010), $(0\bar{1}0)$, $(\bar{1}10)$, and $(1\bar{1}0)$.

(e) Room Temperature Study. A room temperature study showed the cell constants, $a = 10.358(1)$ Å, $b = 15.322(1)$ Å, $c = 7.251(1)$ Å, and $\beta = 98.66(2)°$, to be slightly larger than those at 100 K. In addition, the M−M distance is 3.63(2) Å, and the angles between the plane normals and the M−M vector are 17.54(1)° and 15.56(1)° for the two planes.

$Rb_2[Ni(CN)_4]\cdot H_2O$. The triclinic structure of $Rb_2[Ni(CN)_4]\cdot H_2O$ has columns of $Ni(CN)_4^{2-}$ ions slightly staggered in sets of three and with interstitial Rb^+ ions and water molecules.

(a) $Ni(CN)_4^{2-}$. There are three symmetrically independent anions, those containing Ni1 and Ni2 lying on inversion centers, and that containing Ni3 in a general position. The centrosymmetric anions exhibit deviations from planarity of less than 0.02 Å, while that containing Ni3 is less planar, having N atoms up to 0.063(2) Å out of plane. The mean Ni−C and C−N bond lengths in the Ni1 plane are 1.8685 and 1.158 Å, respectively, in the Ni2 plane they are 1.863 and 1.1615 Å, and in the Ni3 plane they are 1.866 and 1.158 Å, all close to earlier reports.[26,27] Figure 2a shows the arrangement of Ni atoms stacked in approximately linear fashion, with sequence Ni3−Ni1−Ni3−Ni2−Ni3−Ni1−Ni3−Ni2. The Ni−Ni−Ni angles about Ni1 and Ni2 are 180°, since they lie on inversion centers. The Ni2−Ni3−Ni1 angle is 169.76(1)°. The two independent Ni−Ni distances are Ni1−Ni3 = 3.712(1) Å and Ni2−Ni3 = 3.804(1) Å. The average metal chain direction is along the {111} vector. The three anions are approximately parallel, with the Ni3 anion forming dihedral angles of 5.3(1)° with the Ni1 anion and 8.0(1)° with the Ni2 anion. However, all three anions are markedly tilted with respect to the stacking axis. Plane normals form angles with Ni···Ni vectors in the range 17.4(1)−29.2(1)°.

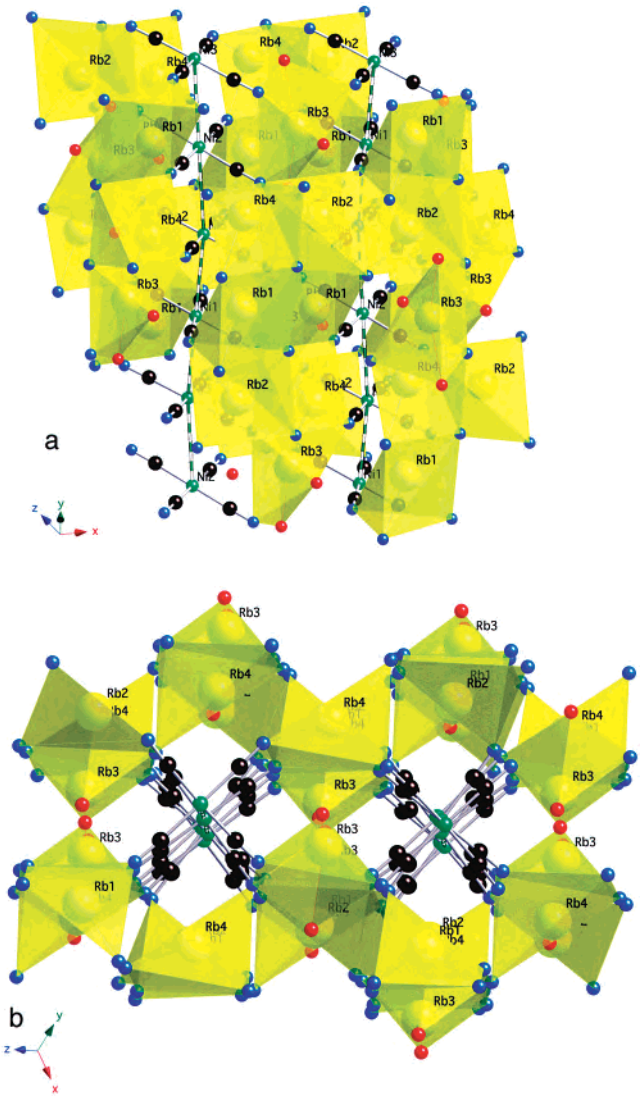

Figure 2. Structure of $Rb_2[Ni(CN)_4]\cdot 1.05H_2O$: (a) side view showing bends in the Ni−Ni chain, (b) = view down $Ni(CN)_4^{2-}$ stack.

(b) Rb^+. All N atoms are coordinated to Rb^+ ions. There are four distinct types of Rb^+ environments, illustrated in Figure 2b. All Rb^+'s are coordinated to N atoms, but only Rb3 is coordinated to any O atoms. The coordination distances are short (2.85−3.09 Å), consistent with those for $Sr[Ni(CN)_4]\cdot 5H_2O$, allowing for the larger ionic radius of

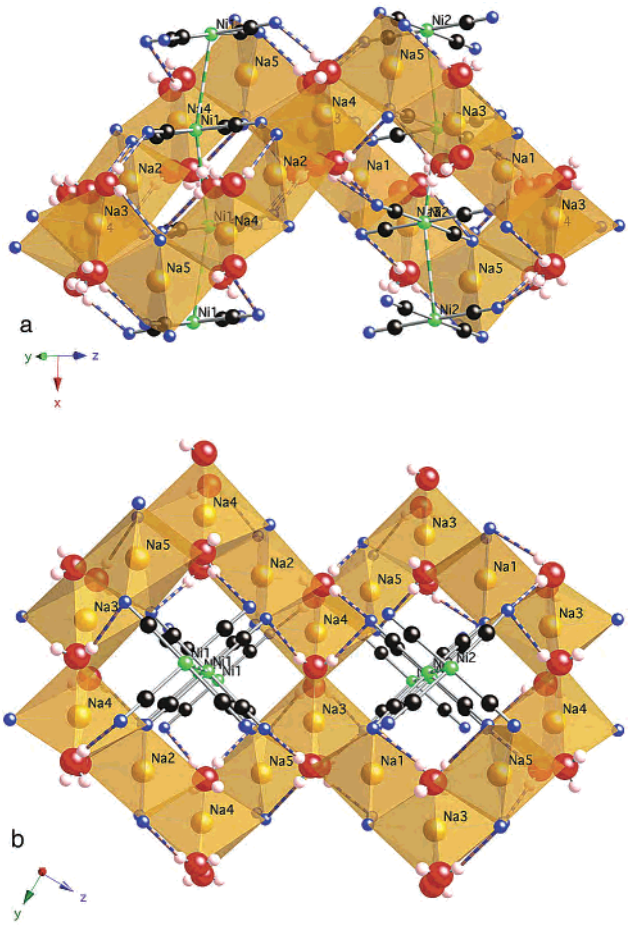

Figure 3. Structure of $Na_2[Ni(CN)_4]\cdot 3H_2O$: (a) side view, showing undulation of connected coordination polyhedra, (b) top view down stacks, showing linking of undulating polyhedra at Na3 and Na4.

Rb^+. Rb1 is coordinated to five N atoms (1, 2, 3, 5, 6); four of the atoms (2, 3, 5, and 6) are essentially in a square arrangement, comprising N's from the Ni1 and Ni3 $Ni(CN)_4^{2-}$ ions in one stack and Ni2 and Ni3 ions in an adjacent stack. The fifth N coordinated to Rb1, N1, is from an Ni1 $Ni(CN)_4^{2-}$ ion in a third stack. This forms a highly distorted trigonal bipyramid and links three separate $Ni(CN)_4^{2-}$ ion stacks together. This Rb1 coordination polyhedron is attached to a polyhedron around Rb2 along the edge straddling two $Ni(CN)_4^{2-}$ columns, at Ni3 and Ni1, and is a distorted tetrahedron with the Rb^+ ion near one edge of the tetrahedron. The Rb2 coordination is thus also to N's in three different $Ni(CN)_4^{2-}$ stacks. One of the N's coordinated to Rb2 (N4) is also coordinated to two other Rb^+ ions: Rb3 and Rb4. The Rb3 coordination is a very distorted octahedron to three O atoms and three N atoms on two different stacks. Rb4 is coordinated to five N atoms from three different stacks.

$Na_2[Ni(CN)_4]\cdot 3H_2O$. There are two $Ni(CN)_4^{2-}$ columns stacked along the *c* axis in a zigzag fashion as shown in Figure 3a. The column containing Ni1 atoms has Ni−Ni−Ni angles of 162.7(1)° and that containing the Ni2's has angles of 165.9(1)°. Between the stacks of $Ni(CN)_4^{2-}$ ions are Na^+ ions and water molecules.

(a) $Ni(CN)_4^{2-}$. Both $Ni(CN)_4^{2-}$ planes are slightly nonplanar with N atoms deviating up to 0.040(1) Å in the anion containing Ni1 and up to 0.081(1) Å in that containing Ni2. These two planes form a dihedral angle of 15.97(2)°. The individual $Ni(CN)_4^{2-}$ planes are tilted from the *a* axis by 10.4(1)° for the Ni1 anion and 20.9(1)° for the Ni2 anion. The mean Ni−C and C−N bond lengths in the planes are 1.8610 and 1.160 Å, respectively. The metal−metal distances are of four lengths: Ni1−Ni1 = 3.684(1) and 3.697(1) Å, and Ni2−Ni2 = 3.620(1) and 3.733(1) Å.

(b) Na^+. There are five different environments for Na^+ ions, each with a slightly distorted octahedral, six-coordinate arrangement: the coordination around Na1, 2, and 5 is to four N atoms and two O atoms and that around Na3 and 4 is to four O atoms and two N atoms. In each coordination octahedron, the N atoms are from two different stacks. The coordination is very tight: for Na−O, it ranges from 2.37 to 2.43 Å, and for Na−N it ranges from 2.46 to 2.60 Å. All coordination octahedra share two edges that contain an O and an N, and in addition, the Na3 and Na4 octahedra are joined along a third edge, sharing two O atoms. The coordination polyhedra thus form chains that undulate through the structure, leaving square channels for the $Ni(CN)_4^{2-}$ ion stacks and joining via the Na3 and Na4 polyhedra to enclose the $Ni(CN)_4^{2-}$ ion stacks. Figure 3b shows a single pair of polyhedra chains around stacks of four Ni1 and four Ni2 planes. Figure 3a shows a side view of the two $Ni(CN)_4^{2-}$ ion stacks with a pair of polyhedra chains surrounding them. All N and O atoms in the crystal are coordinated to the Na^+ anions.

(c) Hydrogen Bonding. There is no O−H···O hydrogen bonding in this crystal and only weak O−H···N hydrogen bonding. Table 3 lists bonding parameters for most of the N atoms, but it is reasonable to assign H-bonding only to atoms 1, 3, 4, 5, and 6.

Spectroscopic Results. The polarized specular reflectance spectra for $Sr[Ni(CN)_4]\cdot 5H_2O$ are shown in the Supporting Information, Figure S1, for $Rb_2[Ni(CN)_4]\cdot H_2O$, in Figure S2, and for $Na_2[Ni(CN)_4]\cdot 3H_2O$, in Figure S3. The corresponding transformed absorbance spectra are shown in Figure 4a−c. Since we are concerned with red-shifting from solution, the polarized solution-equivalent spectra from unperturbed $CsK[Ni(CN)_4]$,[16] which has no apparent solid-state effects, are also shown in each figure. In all solid-state cases for both the *x*,*y*- and *z*-polarized spectra, but much more dramatically in the latter case, there is a red shift from the solution spectral energies. The polarized absorbance spectra have been adjusted to correspond with solution absorbance: the original *z*-polarized spectra have been multiplied by $^1/_3$ and the *x*,*y*-polarized spectra by $^2/_3$ to account for the time-averaged orientations of the chromophores in solution. The *x*,*y*-polarized spectra are nearly identical for the three crystal systems whereas the *z*-polarized spectra are clearly different, reflecting the unique environments on the *z* axes of the molecules as seen in the structural results already described. We will pay close attention to changes in environments in our section describing calculations and in

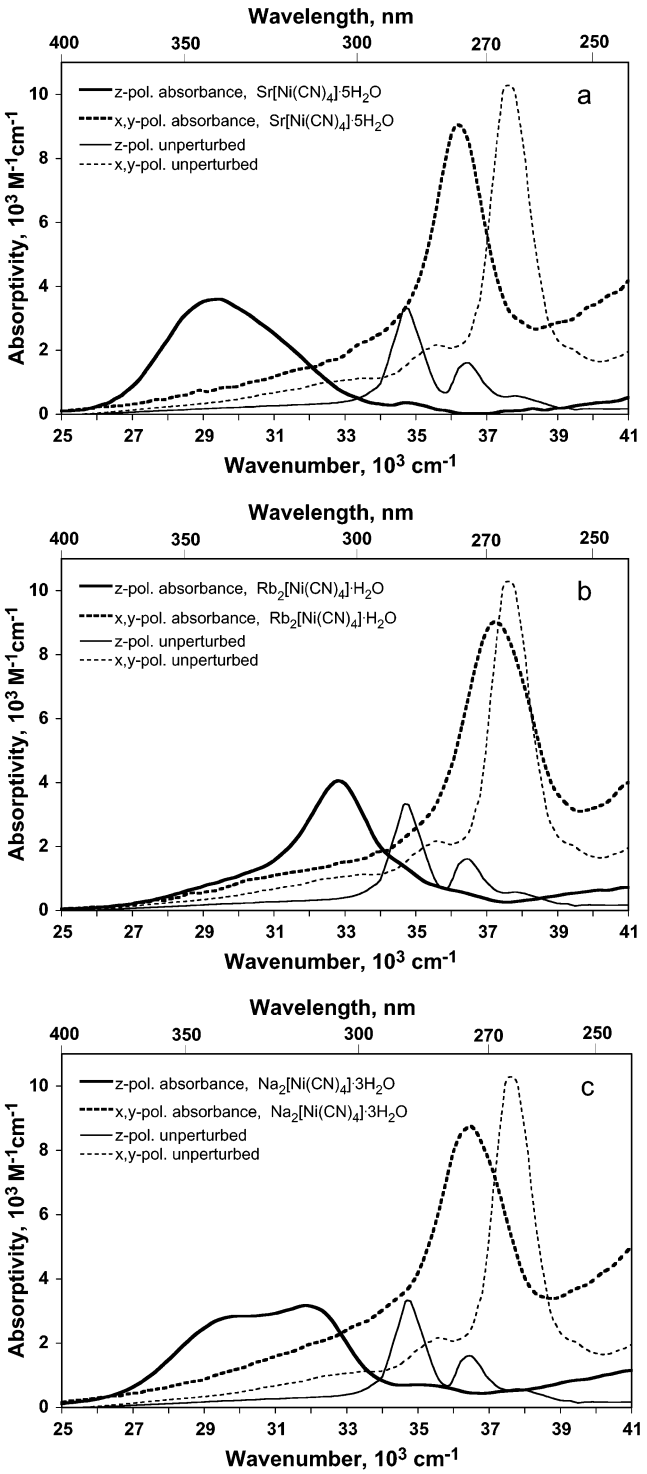

Figure 4. Polarized transformed absorbance spectra compared with polarized spectra having no solid-state effects: (a) $Sr[Ni(CN)_4]\cdot 5H_2O$, (b) $Rb_2[Ni(CN)_4]\cdot 1.05H_2O$, and (c) $Na_2[Ni(CN)_4]\cdot 3H_2O$. Original reflectance spectra are in the Supporting Information.

the discussion of the relationship between the calculated and the experimental results.

In $Sr[Ni(CN)_4]\cdot 5H_2O$, Figure 4a, the spectra were taken off the (110) face; the "*z*-polarized" spectra were taken with the electric vector aligned parallel to the *c* direction and the "*x*,*y*-polarized" were spectra perpendicular to the *c* axis. These are actually about 7° from the molecular *z* and *x*,*y* directions, respectively, but were sufficiently close to the principal dichroic directions to produce apparently clean polarizations. In $Rb_2[Ni(CN)_4]\cdot H_2O$, Figure 4b, the faces of the triclinic crystals were not identified, but the most highly reflective and dichroic face was selected for the spectra and the proper orientations were determined by rotation of the polarizing table while monitoring the reflectance due to the prominent in-plane transition which remained at close to 272 nm. The strongest signal determined the orientation for the *x*,*y*-polarized spectrum, of course, and the *z*-polarized spectrum was obtained at 90° from that orientation. The $Na_2[Ni(CN)_4]\cdot 3H_2O$ crystals were elongated along the *a* axis and were approximately hexagonal prisms. All side faces (i.e., those containing the {100} vector) gave equivalent spectral results, Figure 4c. Again, in these last two cases, the spectral results show that alignment was sufficient to provide good polarization separation.

ZINDO Calculation Results. The purpose of the ZINDO calculations is to model the behavior of the $Ni(CN)_4^{2-}$ ions as their stacking environment changes. Ideally, one would change one variable such as stacking distance to see the results on calculated spectra and their match with experiment. Unfortunately, in the experimental world, the several $Ni(CN)_4^{2-}$ systems available vary not only in stacking distance but also in relative orientation of ligands in adjacent stacks, changing stacking direction (M−M vector) and angle of planar orientation with respect to the stacking vector, or "tilt". We use here the term "straight stack" to designate molecular planes oriented 90° from the M−M vector and "tilted stack" to indicate a non-90° angle between planes and the M−M vector. An extreme case of tilted stacking and changing M−M vectors was found in $Cs_2[Ni(CN)_4]\cdot H_2O$ where the $Ni(CN)_4^{2-}$ planes are arranged helically around a central axis.[10] We have selected a subset of orientations for this paper in which the ligands are eclipsed, but as was shown in the section describing structure results, the orientations differ in more ways than the stacking distance between planes. We have begun calculations with the simplest model, a straight stack.

In our work on a single $Ni(CN)_4^{2-}$ ion,[26] we showed that good agreement with experimental spectra and with ab initio orbital energy calculations is possible if the bonding parameters are $\beta_{s,p} = -5$ and $\beta_d = -41$ and configuration interaction includes the top 10 filled and lowest 10 virtual orbitals ("CI level" = 10). The prominent *x*,*y*-polarized state transition, $A_{1g} \rightarrow E_u$ (e_g (d_{xz}, d_{yz}) → a_{2u} (p_z, π^*)), was found to consist of several orbital transitions. One of the degenerate transitions was found to be $-0.97(2e_g \rightarrow 4a_{2u}) - 0.07(1e_g \rightarrow 3b_{2g}) + 0.06(2b_{2g} \rightarrow 9e_u) + 0.18(1e_g \rightarrow 4a_{2u})$ while the *z*-polarized state transition was simply one orbital transition, $9a_{1g} \rightarrow 4a_{2u}$. In the subsequent paper, on $Cs_2[Ni(CN)_4]\cdot H_2O$,[10] we showed that each of the component orbitals involved in the single ion transitions combined three ways to provide a plethora of orbital transitions for a model of three ions stacked in the helical arrangement. We also did not neutralize the ionic charges, recognizing that the orbital energies in a collection of several ions were not realistic, but that the transition energies were not largely affected, as judged by the agreement with experiment.

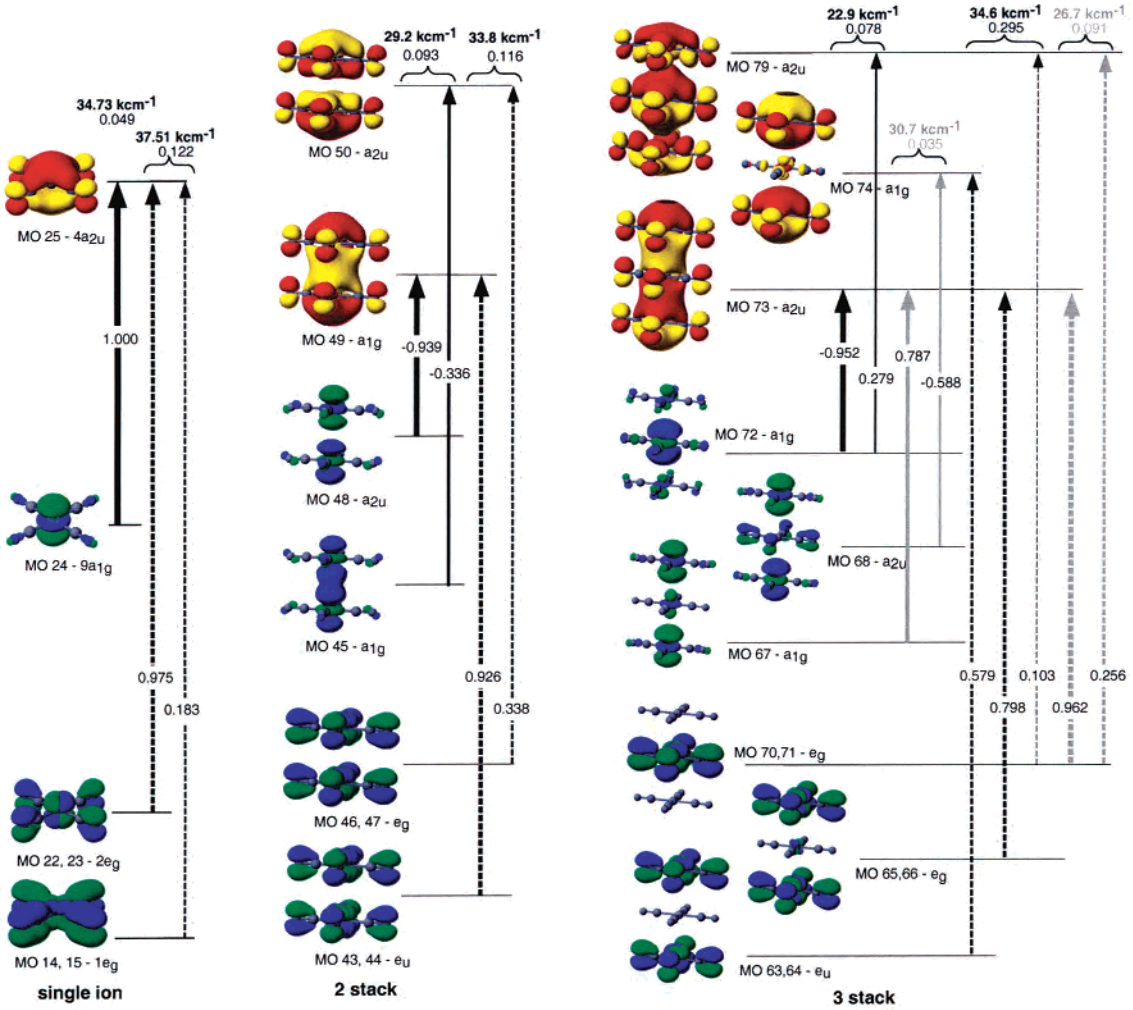

Figure 5. Molecular orbitals and orbital transitions involved in state transitions for various aggregations at an M−M distance for 2 and 3 stacks of 3.63 Å. Transitions: — = *z* and - - - = *x*,*y*-polarized; gray = less intense state transitions.

Result of Increasing Aggregation. We now examine the process of aggregation in detail, and we will begin with a straight stack, with the planes aligned so that the ligands are eclipsed as they are experimentally in the three salts under study. Perfectly symmetric $Ni(CN)_4^{2-}$ ions were chosen, with Ni−C and C−N bond lengths of 1.860 and 1.154 Å corresponding essentially to the average bond lengths in Sr-$[Ni(CN)_4]\cdot 5H_2O$ and angles Ni−C−N of 180° and C−Ni−C of 90°. The straight and eclipsed arrangements allow the D_{4h} molecular point group to be retained at any degree of aggregation. Using $\beta_{s,p} = -5$ and $\beta_d = -41$, we began aggregating $Ni(CN)_4^{2-}$ planes. For two planes, the optimal CI level is 20 for the pair since there are twice as many orbitals involved in the transitions of interest. The orbitals involved in the principal state transitions are illustrated in the center portion of Figure 5. It is reassuring to note that the molecular orbitals are essentially a linear combination of the single-molecule molecular orbitals: two single-ion $4a_{2u}$ orbitals combined into an a_{1g} (MO 49) and an a_{2u} (MO 50) orbital, two $9a_{1g}$ orbitals combined into an a_{1g} (MO 45) and an a_{2u} (MO 48) orbital, and the $2e_g$ pair (MO 22, 23) combined into an e_g pair (MO 46, 47) and an e_u pair (MO 43, 44). The *z*-polarized state transition resulting from this aggregation at a stacking distance of 3.63 Å had an energy of 29.2 kcm^{-1} with an oscillator strength of 0.093 (adjusted to a per molecule basis), compared with the single-ion transition energy of 34.7 kcm^{-1} and oscillator strength of 0.049. It is composed of essentially two orbital transitions (comprising 99.5% of the state transition intensity from the sum of squares of coefficients) as shown in Figure 5. Regarding the *x*,*y*-polarized transition, while primarily two pairs of MOs were involved in the single-molecule state transition at 37.5 kcm^{-1}, only orbitals based upon the higher-energy pair, the $2e_g$, are significant contributors to the *x*,*y* transition in the two-plane stack (although orbitals based on the $1e_g$ pair do contribute also, consistent with linear combination of orbitals). Not inconsistent with our assignment in mixed Ni/Pt tetracyano crystals, we point out that the two-stack derivatives of the single dianion $2b_{2g}$ orbital, MOs 41 and 42, and of the $9e_u$ pair, MOs 56 and 58, also contribute albeit in a very minor (<1%) way as transitions 41 → 56 and 42 → 58. If it were possible to construct a realistic computer model with Pt doping, it would be interesting to explore the contribution of these orbitals further. A detailed listing of orbital transition components is given in the Supporting Information, Table S-1. The results

in Figure 5 show that, even for two planes, this linear combination of orbitals model produces a red shift and an increase in intensity as was seen experimentally (Figure 4).

For the three-plane case, the results become a bit more complex. As expected, three molecular orbitals are formed from each of the single-molecule orbitals of interest here: as illustrated in the right side of Figure 5, two a_{2u} orbitals (MO 73 and 79) and one a_{1g} orbital (MO 74) are formed from three single-ion $4a_{2u}$ orbitals, and a similar situation develops from the single-ion $9a_{1g}$ and $2e_g$ orbitals. In each case, a typical linear combination of orbitals has occurred: the lowest energy MO has no nodal planes between Ni atoms, the intermediate one has essentially one node, and the highest energy MO (79) has two nodal planes introduced by the LCMO model. At a separation of 3.63 Å, two *z*-polarized state transitions develop, both red-shifted from solution, a strong transition (osc str = 0.078) at 22.9 kcm^{-1} and a weaker one (osc str = 0.035) at 30.7 kcm^{-1}. The two most significant orbital transition components for each state transition are shown in Figure 5; a complete listing of those comprising at least 98% of the transition intensity is provided in Table S1.

The *x*,*y*-polarized transitions follow a pattern similar to that of the *z*-polarized transitions. The most intense state transition consists of transitions from the orbitals deriving only from the higher energy π orbital pair (MO 22,23) in the single-ion model. The weaker of the two state transitions, the peak at 26.7 kcm^{-1}, follows the *z*-polarized case in which the largest orbital transition contribution is from an "inner orbital" to the lowest-energy delocalized a_{2u} orbital. The much stronger of the state transitions, however, involves primarily the e_g and e_u "outer orbitals" in the three-molecule stack.

Effect of Stacking Distance. The next feature we will illustrate is the effect of stacking distance on the energy of the two types of transitions, those deriving from the *z*-polarized and the *x*,*y*-polarized single-molecule transitions. We used the three-stack model because of our confidence in its validity due to our experience with $Cs_2[Ni(CN)_4]\cdot H_2O$[10] and the more realistic modeling of the crystalline stack than by the two-stack model. For this illustration, we retained the straight-stacking configuration as used in the study of aggregate size and the bonding parameters $\beta_{s,p} = -5$ and $\beta_d = -41$ as used in our previous two studies.[10,26] Figure 6 shows the results of calculations of stacking distances from 6.5 to 3.63 Å along with the experimental energies for the corresponding transitions in the polarized single-molecule case.[16] The thickness of lines represents the relative oscillator strengths of the four peaks calculated. The principal result is that the model depicts a red shift upon a reduction of stacking distance, in agreement with experiment.[39−45] The

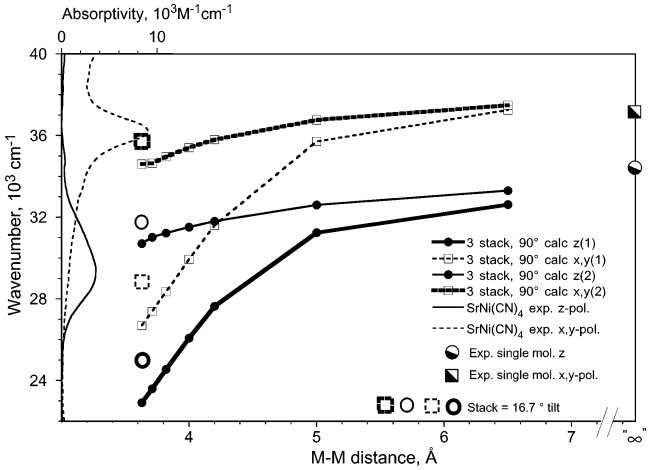

Figure 6. *E* vs M−M distance for calculated ($\beta_{s,p} = -5$, $\beta_d = -41$) 3 stack eclipsed model, with tilted (3.63 Å), single-molecule, and $SrNi(CN)_4$ experimental spectra.

other significant result is that, for each polarization, one of the state transitions is much more intense than the other one of the same polarization: the higher-energy *x*,*y*-polarized transition and the lower-energy *z*-polarized transition. The results from the experimental work presented in this paper and from other work[9,10,15,17] show that the *x*,*y*-polarized transition has much less red-shifting than does the *z*-polarized transition. This is also the result for the more intense of the calculated transitions.

Our interim conclusion is that the linear combination of atomic orbitals model contains components that follow the experimental solid-state perturbation behavior for both polarizations in tetracyanonickelates. Our tentative conclusion regarding relative transition intensities, based on the three-plane stack, is that this model also leads to the experimental result that the state transitions may be described reasonably well using an orbitally based model as opposed to a band-based model. The band-based model[24] would lead to a broad absorption in the low energy region and a high metallic-appearing reflectance from the low visible through the IR;[11] the sharp peak that red shifts and grows in intensity as stacking becomes closer and the nonmetallic appearance of the crystals are reasonable evidence of a nonband mechanism. The sharp peak at the low energy end is reminiscent of exciton formation[25] which has been used for many years successfully, especially with solid-state organic molecules.[46,47] On the other hand, the application of ZINDO to crystalline benzene by Zerner et al.[48] did not produce a satisfactory match to experiment while exciton theory does describe the crystalline spectrum very well. At this time, we are investigating further the correlation, if any, between the results from the LCAO approach of routines such as ZINDO and exciton theory, but at present, we suspect that the treatments and, by implication, the mechanisms in systems well-described by the two are not equivalent.

(39) Yersin, H.; Gliemann, G. *Z. Naturforsch., B: Chem. Sci.* **1975**, *30*, 183.
(40) Yersin, H.; Gliemann, G. *Ann. N.Y. Acad. Sci.* **1978**, *313*, 539.
(41) Lechner, A.; Gliemann, G. *J. Am. Chem. Soc.* **1989**, *111*, 7469.
(42) Cowman, C. D.; Ballhausen, C. J.; Gray, H. B. *J. Am. Chem. Soc.* **1973**, *95*, 7873.
(43) Moreau-Colin, M. L. *Bull. Soc. Chim. Belg.* **1965**, *51*, 916.
(44) Moreau-Colin, M. L. *Bull. Soc. Chim. Belg.* **1965**, *34*, 772.
(45) Moreau-Colin, M. L. *Struct. Bonding (Berlin)* **1972**, *10*, 167.
(46) Fox, D.; Schnepp, O. *J. Chem. Phys.* **1955**, *23*, 767.
(47) Albrecht, A. C.; Simpson, W. T. *J. Chem. Phys.* **1953**, *21*, 940.
(48) Coutinho, K.; Canuto, S.; Zerner, M. C. *Int. J. Quantum Chem.* **1997**, *65*, 885.

Effect of Tilting. All three crystal systems reported here contain some sort of a tilt of the stacking chain with respect to the Ni−Ni vectors; the most regular arrangement is that in $Sr[Ni(CN)_4]\cdot 5H_2O$. In modeling this system in which the planes have a 16.6° average tilt from normal to the stacking direction at room temperature, we looked at the effect of this tilt on the calculations. Figure 6 includes two open squares and two open circles depicting the energies of the four peaks of interest upon a 16.7° tilt in the stacking chain from normal with a Ni−Ni distance of 3.63 Å. From Figure 5, one is able to see that a tilt would not affect the binding orbitals, which do not overlap, but would decrease the overlap of the binding regions of the virtual orbitals, raising their energy which may qualitatively account for the greater transition energies; we emphasize, however, that transition energies are not simply the difference of orbital energies.[32] This effect is comparable to increasing the stacking distance: the peaks are about 2 kcm^{-1} less red-shifted than the corresponding straight-stacked 3.63 Å peaks.

From Figure 4a, one can see that experimentally there is a *z*-polarized transition at about 29 kcm^{-1} and an *x*,*y*-polarized transition at about 36 kcm^{-1}, representing a significant red shift of the *z*-polarized transition and a slight red-shift of the *x*,*y*-polarized prominent peak. This information has been superimposed on the far left in Figure 6 to allow comparison between experimental results and the calculations (with $\beta_{s,p} = -5$ and $\beta_d = -41$) to this point. It is clear that the red shift is generated for all four calculated state transitions (*z*(1), *z*(2), *x*,*y*(1), and *x*,*y*(2)). As noted in an earlier paragraph, the more intense *x*,*y*-polarized transition, *x*,*y*(2), produces a much better match to experiment than *x*,*y*(1), especially when the experimental tilt of 16.7° is accounted for. This is depicted by the bold dashed square in Figure 6. Neither of the tilted *z*-polarized transitions (circles at left in Figure 6) show as good agreement as *x*,*y*(2), and it is unclear which one is better. While both the single-molecule[26] and three-molecule helical models (Ni−Ni−Ni = 155° and Ni−Ni = 3.55 Å)[10] show excellent agreement with experiment using $\beta_{s,p} = -5$ and $\beta_d = -41$, the axial approach in the present crystal structures is different (Ni−Ni−Ni = 180° and Ni−Ni = 3.63 Å) with adjacent planes parallel to each other, allowing more interaction between axial orbitals and adjacent planes. Since the values of $\beta_{s,p}$ and β_d relate to the orbital overlap between the Ni s,p and d orbitals respectively, on the metal with ligand orbitals, it seems wise to examine the effect on spectra of varying β values.

Variation of Bonding Parameters (*β*'s). Figure 7 shows the energies of the two best calculated state transitions (*z*(1) and *x*,*y*(2)) as functions of $\beta_{s,p}$ and β_d with a planar tilt of 16.7°. One can see that $\beta_{s,p} = -5$ and $\beta_d = -41$ yield good agreement with the experimental *x*,*y*-polarized peak for $Sr[Ni(CN)_4]\cdot 5H_2O$ and that the other values of $\beta_{s,p}$ and β_d are less satisfactory. On the other hand, this set of β parameters is apparently not as valid for the *z* polarization. Looking at the calculated results in Figure 7, it appears that three sets of $\beta_{s,p}$ and β_d yield reasonable energies for the transition: $\beta_{s,p} = -5$ and $\beta_d = -80$, $\beta_{s,p} = -4$ and $\beta_d = -61$, or $\beta_{s,p} = -3$ and $\beta_d = -41$. Thus, because only one set of β values is formally allowed within the ZINDO theory formulation[49] that describes electronic transitions, a tradeoff appears necessary that results in the smallest sum of deviations of the two calculated maxima from the experimental peak positions. In addition, a couple of constraints are necessary that result from an attempt to base our choice on consistency with the available experimental data.

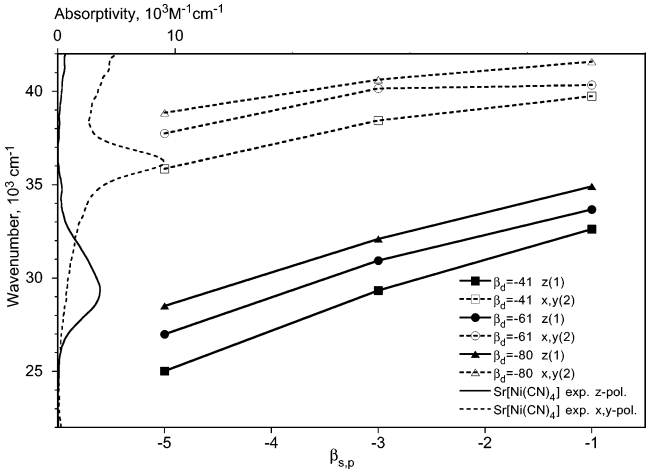

Figure 7. *E* vs β values for the 3 stack eclipsed model (M−M = 3.63 Å, tilt = 16.7°) and $SrNi(CN)_4$ experimental spectra.

As shown in Figure 7 and in our prior work on the single ion,[26] an increased magnitude of $\beta_{s,p}$ for $Ni(CN)_4^{2-}$ seems justified. However, the default ZINDO value (−1)[38] yields the best spectral agreement for a number of other compounds, including a member of the Ni porphyrins, octaethylporphrinatonickel (Ni(OEP)).[50] A relatively larger value of $\beta_{s,p}$, which by definition results in a greater Ni s,p overlap with neighboring orbitals, would be expected for compounds that have shorter experimental Ni−ligand bond lengths. The increased magnitude of $\beta_{s,p}$[10,26] over that used for porphyrins (−1) is consistent with greater Ni s,p overlap with ligands in $Ni(CN)_4^{2-}$ than between Ni s and p orbitals in Ni porphyrins. In fact, the Ni−C distance in $Sr[Ni(CN)_4]\cdot 5H_2O$ is 1.858 Å, while the corresponding Ni−N distance is appreciably larger, 1.958 Å, in Ni(OEP).[51] Thus, our choice of a greater value of $\beta_{s,p}$ seems justified. Figure 5 shows that the virtual orbitals primarily involved with both the *z*- and *x*,*y*-polarized transitions derive from the $4a_{2u}$ orbital in the single molecule. This orbital can be seen to have a significant Ni pz−C pz overlap and has a 36% contribution from the metal pz orbital. On the other hand, a ZINDO calculation on Ni(OEP) shows that, for the orbitals involved in the state transitions commonly referred to as the "Q" and "B" or "Soret" *x*,*y*-polarized transitions, there is at most 1.3% Ni pz contribution.[50] Furthermore, the optimal value of β_d is expected to be at least as large as that for the single ion, given that the Ni−Ni separation of 3.567 Å is smaller than that in the unperturbed CsK system with essentially non-interacting adjacent planes separated by 4.3 Å.

(49) Bacon, A. D.; Zerner, M. C. *Theor. Chim. Acta* **1979**, *53*, 21.
(50) Evans, J. S.; Musselman, R. L. *J. Am. Chem. Soc.*, submitted.
(51) Meyer, E. F. J. *Acta Crystallogr.* **1972**, *B28*, 2162.

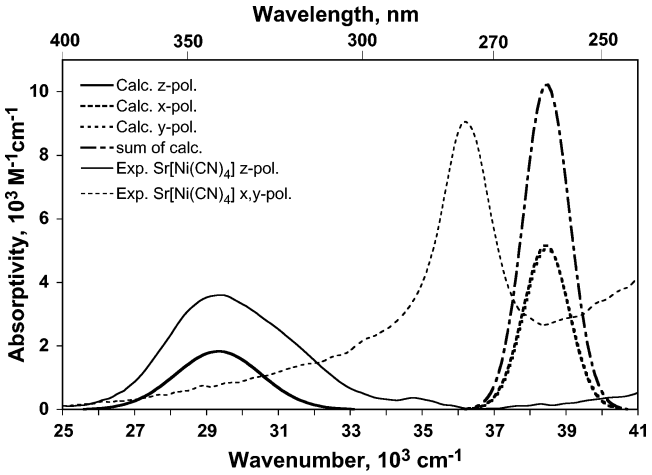

Figure 8. Calculated spectra with experimental absorbance spectra for $Sr[Ni(CN)_4]\cdot 5H_2O$.

With these considerations in mind, we thus propose a single set of parameters, $\beta_{s,p} = -3$ au and $\beta_d = -41$ au, to describe both polarization transitions in the 3-ion stack eclipsed model. This choice yields the best simultaneous agreement of both polarizations with experiment. The resulting calculated spectra are depicted in Figure 8. In both cases, predicted peak positions lie within 2 kcm^{-1} of experiment, while relative intensities agree quite well; absolute intensities agree semiquantitatively. Overall, the agreement is satisfactory.

As a technical aside, we note that the *z*-polarized transition involves orbitals derived primarily from the $9a_{1g}$ single-molecule orbital, which consists of 88.5% Ni d_{z^2}. The *x*,*y*-polarized transition, on the other hand, is described by the degenerate pairs MO 63, 64, MO 65, 66, and MO 70, 71, all of which are based on the single-molecule $2e_g$ orbital that is formed primarily (76%) from Ni d_{xz} and Ni d_{yz} orbitals. One would predict that a larger value of β_d would cause greater repulsion in nodal regions but simultaneously stabilize to a greater extent MOs with d_{z^2}-orbital character, resulting in a more rapid energy increase of the *z*-polarized transition, which in fact is observed in Figure 7. In the defining eq 16 of Bacon and Zerner's pioneering work,[49] the resonance integral, $\beta_{\mu\nu}$, is equal to the product of the "average" bonding parameter and the weighted overlap integral, $\bar{S}_{\mu\nu}$, which contains distinct terms to account for σ or π orbital overlap. The extent of σ or π orbital overlap is controlled by adjusting these empirical interaction factors. Due to the σ character of one set of MOs (those associated with the *z*-polarized transitions) in this work compared to the ligand π character of the other set of MOs (those associated with the *x*,*y*-polarized transitions), we hypothesize that it may be possible to vary these empirical factors/degrees of freedom to achieve an excellent match of both *z*-polarized and *x*,*y*-polarized transition energies with experiment. Mathematically, this is equivalent to selecting different β_d's in Bacon and Zerner's eq 16. We thus point out that it may be reasonable to fit each polarization transition with its own set of β parameters. For example, the best values for the *x*,*y*-polarized transition are $\beta_{s,p} = -5$ and $\beta_d = -41$, while those for the *z*-polarized peak are $\beta_{s,p} = -5$ and $\beta_d = -80$. We are currently investigating whether this loophole actually does exist in the ZINDO theory, that is, whether changing the σ and π interaction factors for a given set of β parameters, which would yield a single set of MOs, results in the same spectrum as selecting multiple sets of β parameters, which yields multiple sets of MOs that cannot coexist and are thus unphysical.

The other crystal structures involve alternating angles and tilts in the stacking orientation of the planes and thus present a more complex electronic environment. This is reflected especially in the spectrum of $Na_2[Ni(CN)_4]\cdot 3H_2O$ where two *z*-polarized peaks appear in the 29−33 kcm^{-1} region. We have not attempted to model the more complicated stacking arrangements due to the difficulty of modeling varying patterns with a stack segment of only three molecules.

Conclusions

We have presented the crystal structures of three $Ni(CN)_4^{2-}$ salts all with eclipsed ligands. The absorption spectra of all three salts show a slight red shift in their *x*,*y*-polarized absorption spectra and a large red shift in their *z*-polarized absorption spectra upon crystallization from solution. The simple linear combination of atomic orbitals used in semiempirical ZINDO calculations provides a sufficiently accurate model of the solid state, even with only a three-molecule segment, to reproduce the red-shifting and intensity increase found experimentally upon crystallization. The modified nickel $\beta_{s,p}$ bonding parameter value of −5 found appropriate for Ni coordination in previous studies of single-molecules[26] and a helically stacked crystal[10] was reduced in absolute value to −3 for the more parallel-stacked $Ni(CN)_4^{2-}$ planes here, while β_d was retained at −41. The planes are not sufficiently close to produce the metallic reflectance characteristic of band formation, and the sharp low-energy peaks also suggest a nonband mechanism is present. The "solid-state effect" present in this set of moderately spaced square-planar complexes thus may adequately be described as due to linear combination of atomic orbitals in at least several planes along the stacked chain and the linear combination of several orbital transitions (configuration interaction-singlets) among the resultant molecular orbitals near the Fermi level.

Acknowledgment. The authors are grateful to the Research Corporation and the National Science Foundation (CHE9521548) for grants to R.L.M. We thank S. Mayer for the preparation of $Na_2[Ni(CN)_4]\cdot 3H_2O$, R. Trapp, Jr., for the preparation of $Sr[Ni(CN)_4]\cdot 5H_2O$, and Prof. C. Larochelle of Franklin and Marshall College for helpful discussions.

Supporting Information Available: Complete crystallographic data in CIF format, reflectance spectra, a table of orbital transition components and parameters of calculated state transitions, sample output for the 123 MOs of a straight stack of three molecules, and graphical depiction of the orbitals. This material is available free of charge via the Internet at http://pubs.acs.org.

IC0345222